ISTITUTO NAZIONALE DI FISICA NUCLEARE

Sezione di Bari

INFN/AE-83/4
12 Aprile 1983

M. De Palma, C. Favuzzi, G. Maggi, E. Nappi, A. Ranieri
and P. Spinelli: MEASUREMENT, PARAMETRIZATION AND FAST SIMULATION OF HADRONIC SHOWERS IN LEAD

Servizio Documentazione
dei Laboratori Nazionali di Frascati

Istituto Nazionale di Fisica Nucleare
Sezione di Bari

INFN/AE-83/4
12 Aprile 1983

MEASUREMENT, PARAMETRIZATION AND FAST SIMULATION OF HADRONIC SHOWERS IN LEAD

M. De Palma, C. Favuzzi, G. Maggi, E. Nappi, A. Ranieri and P. Spinelli
Dipartimento di Fisica dell'Università di Bari, and INFN, Sezione di Bari

(Submitted to Nuclear Instruments and Methods)

ABSTRACT

Measurements on longitudinal and lateral hadronic shower development in lead at 13 and 20 GeV are presented. It is shown that the longitudinal shower profile can be parametrized by a two component formula. A fast hadronic shower simulation method based on parametrization is described together with a possible method to introduce fluctuation in the shower development. A comparison between the simulation and data is also presented.

1. - INTRODUCTION

At present many elaborate and accurate hadronic shower simulation programs exist[1,2]. These are very useful in predicting calorimeter responses, nonetheless they are time-consuming even with powerful computers, since they simulate shower development by following the interactions of each particle produced.

A fast hadronic shower simulation giving the calorimeter gross behaviour can be more interesting than the ones studying the shower development complete details especially when some properties of the apparatus, for example its resolution, are already known.

In this paper we present a method to simulate hadronic shower response of the calorimeter used in the NA 24 experiment[3] at CERN. This calorimeter consists of two

photon-hadronic modules, known as ring and downstream calorimeter[4], used in the NA 5 experiment and of a high resolution photon position detector (PPD). The PPD[5], which covers the ring calorimeter front active face, consists of 8 lead sheets sandwiched with a total of 12 layers of proportional aluminium tubes amounting to 9.6 radiation length. The ring calorimeter[6], a barrel 3 m in diameter with a 56 cm central hole, has a lead-scintillator sandwich photon section (16 x 0.56 cm of Pb-sheets) followed by an iron-scintillator sandwich hadronic section (22 x 5 cm of Fe-sheets). Both sections are subdivided into 24 sectors and 10 rings for a total of 240 independent cells, each substending about 9^{o} in the c.m. polar angle and 15^{o} in the azimuthal angle. For both sections, the output signal from each cell is proportional to the longitudinal integrated energy deposition[7]. The downstream calorimater has a similar longitudinal structure and covers the central hole of the ring calorimeter.

In this kind of detector, the hadronic shower can start either in the lead of the PPD or in the photon section of the ring calorimeter and then develop in the following sections. The incident energy is thus shared among the three different detectors: the PPD, the photon section and the hadronic section of the ring calorimeter. In order to evaluate the fraction of energy released in each detector, the hadronic shower shape in the different materials, i.e. lead and iron, must be known.

While several measurements of hadronic shower development, at a fixed origin, in iron can be found in literature[8, 9], fewer data exist for hadronic shower development, at a fixed origin, in lead[10]. The latter has been determined by us at 13 and 20 GeV with a fine sampling (1 X_o).

The paper is organized as follows: section two describes hadronic shower development in lead; section three presents a parametrization of the longitudinal profile of the type suggested by Bock et al.[10]; section four deals with shower fluctuation in lead and section five illustrates the method used to simulate the response of the ring calorimeter and shows simulation results.

2. - SHOWER STUDY

2.1. - Description of the experimental set-up

The experimental set-up (Fig. 1) used for shower development measurements consisted of 16 square lead plate (each having a side of 40 cm and a thickness of 0.56 cm) spaced by 2 cm, four NE-110 plastic scintillator counters of size $30 \times 30 \times 0.8$ cm^3 (B--counters), used to sample the longitudinal energy deposition, six NE-110 counters of size $3.5 \times 30 \times 0.8$ cm^3 (F-counters), assembled together in an array covering 30 x 21

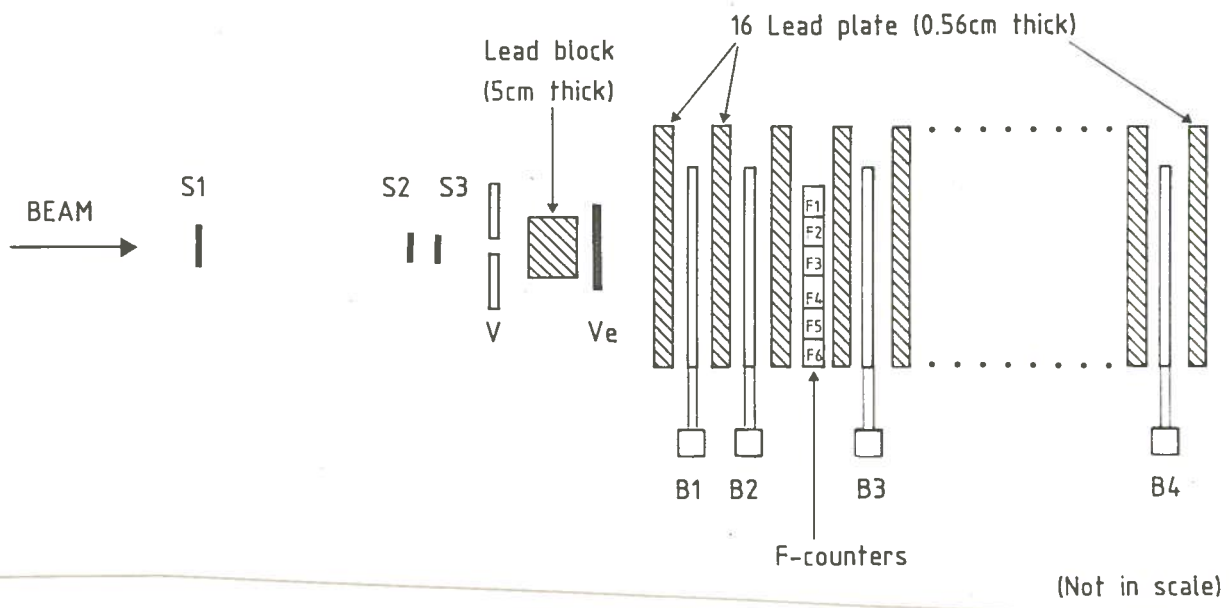

FIG. 1 - Side view of experimental set-up. B3, B4 and F counters were located in different positions along the lead planes to sample the shower development at different depth.

cm^2, used to study lateral shower development.

All the B and F counters were wrapped with aluminum foil and were connected to a photomultiplier by a suitable plexiglass light-guide. The light attenuation of the counters was measured and the non-uniformities were found to be at most 2%.

The B-counters were equipped with 56 AVP photomultipliers while the F-counters were equipped with XP 2008 photomultipliers.

The output from each B-counter was split into two signals: one was sent to the trigger logic, the other to the ADC's, while signals from the F-counters were sent directly to the ADC's.

Scintillator counters, V, S1, S2, S3, Ve were installed in the beam line as shown in Fig. 1. V is a veto counter with a 1 cm diameter hole at the center, S1 (1×2 cm^2), S2 (1×1 cm^2), S3 (1×1 cm^2) are three small beam-defining counters. The coincidence $\bar{V} \cdot S1 \cdot S2 \cdot S3 = Beam$ defines an incoming particle. The Ve (20×20 cm^2) counter, placed behind a 5 cm thick lead block, was used in the trigger to veto early produced showers so as to remove electron contamination from the hadron beam. The Ve signal was also read out by an ADC.

Data were taken at two different energies, 13 GeV and 20 GeV, with a negative beam consisting mostly of pions, at CERN PS.

2. 2. - Trigger definition

The B, F and Ve counters were calibrated in terms of number of equivalent particles (e. p.). The e. p. can be defined the most probable energy loss in the counter by a beam particle (b. p.). A typical b. p. pulse-height distribution is shown in Fig. 2.

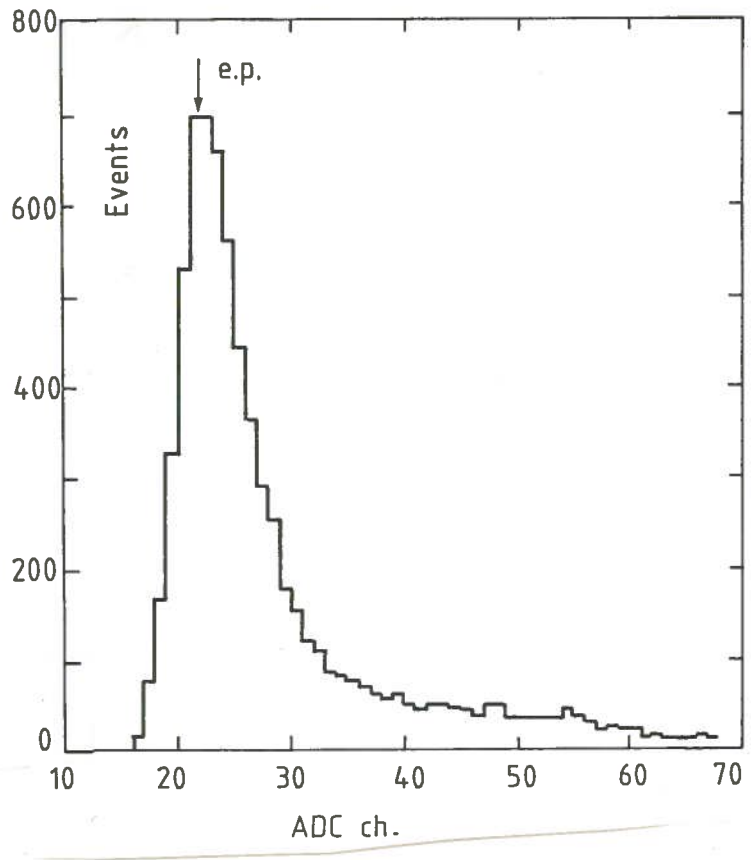

FIG. 2 - Typical pulse-height distribution for beam particle (for B counter). The arrow 'e. p.' shows the most probable pulse--height.

The most probable pulse-height was evaluated by using the average pulse-height for channels with counts above 50% of the highest count value, and then correcting the mean with the following formula[8]:

peak = mean - 0.25 • standard deviation.

Different runs were taken for the two beam energies. The discrepancies found remain within uncertainty in the definition of e. p. ($\sim$ 1%).

Since hadronic showers starting in the first plate of the lead are the main concern of the study, in order to remove electron initiated showers from our sample, we selected those beam particles which had in Ve, i. e. after traversing 5 cm of lead, a b. p. signal. This selection was made by setting the Ve discrimination threshold just below the two e. p. level and by using its output to veto the beam defining logic.

Only about 25% of the pions interacted in the lead block, however, we had enough coincidence Beam • $\overline{(Ve > th)}$ ($\sim$ 10 K p. p. s.) having an electron contamination estimated less than 0.1%.

In order to select the hadronic showers starting in the first plate, the B1 and B2 counters, placed after the first and the second lead plate respectively, must detect more than one particle. To achieve this the B1 and B2 signals were sent to two discriminators with the threshold set just below the two e. p. signal. Therefore, the coincidence Beam • • $\overline{(B1 > Th1)}$ • $\overline{(B2 > Th2)}$ • $\overline{(Ve > Th)}$ ($\sim$ 100 p. p. s.) defines an incoming hadron having its first interaction in the first lead plate and it was used as trigger.

In order to sample the shower development at various depths, B3, B4 and the F--counters were located at different positions along the 16 lead plates. For each position, 10. 000 events were recorded and the beam was centered between the F2 and F3 counters.

2. 3. - Data analysis

The event recorded results still contamined by particles which do not shower, but

is strongly related to the position of the shower maximum and that our data reproduce better the region around the maximum, owing to the finer sampling. Lacking sufficient data on the shower tail, in a subsequent fit we assumed the β_H parameter from ref. (10). This parameter is related to the shower tail. The minimization gives, with an average $(dep_{meas}(x) - dep_{fit}(x))^2/\sigma^2 = 2.7$, the following set of parameters:

$$\alpha_E = 0.946 + 0.618 \log E , \qquad \alpha_H = 0.974 + 0.068 \log E ,$$

$$\beta_E = 0.290 , \qquad \beta_H = 0.9099 + 0.0237 \log E \quad \text{(ref. (10))} ,$$

$$w = 0.464 .$$

The solid line in Fig. 4 shows the fit for both energies.

As a check these parameters were used to reproduce the shower development in iron (data from ref. (8)). Since these data refer to showers originating in the first 9-30 cm of the iron, the shower origin is generated according to the density distribution $f(x) = \exp(-x/\lambda_{ab})/\lambda_{ab}$ in the range from 9 to 30 cm. Fig. 7 reports the measured and the simulated longitudinal shower profiles in iron.

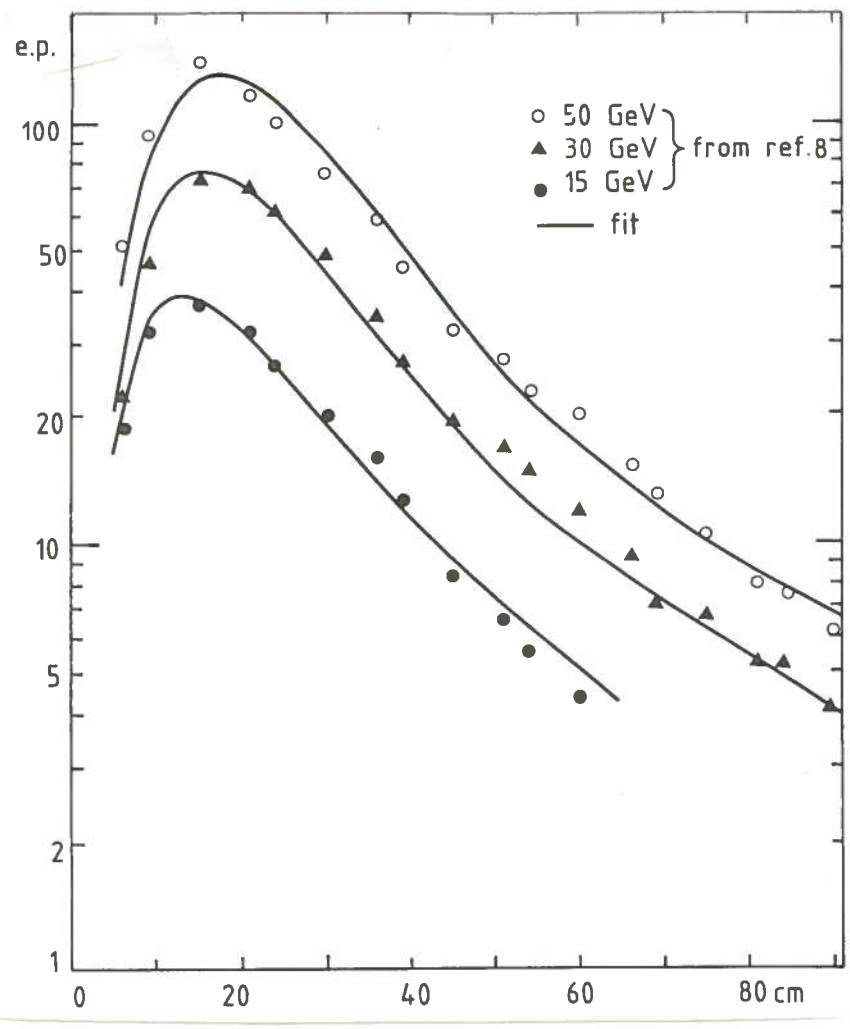

FIG. 7 - Longitudinal shower development in iron. The solid line shows the results of the simulation described in the text.

4. - FLUCTUATIONS OF THE SHOWER LENGTH

It was observed[12] that the hadronic showers have an approximate universal longitudinal profile when the longitudinal dimensions is scaled according to the their center of gravity.

Therefore, the shower length fluctuations may be related to the center of gravity distribution. This distribution is known for iron[8]. The integral distribution of the f ratio of the center of gravity of a generic shower to the center of gravity of the mean shower for 15 and 75 GeV energies is plotted in Fig. 8. This figure shows that the distribution is independent of the energy.

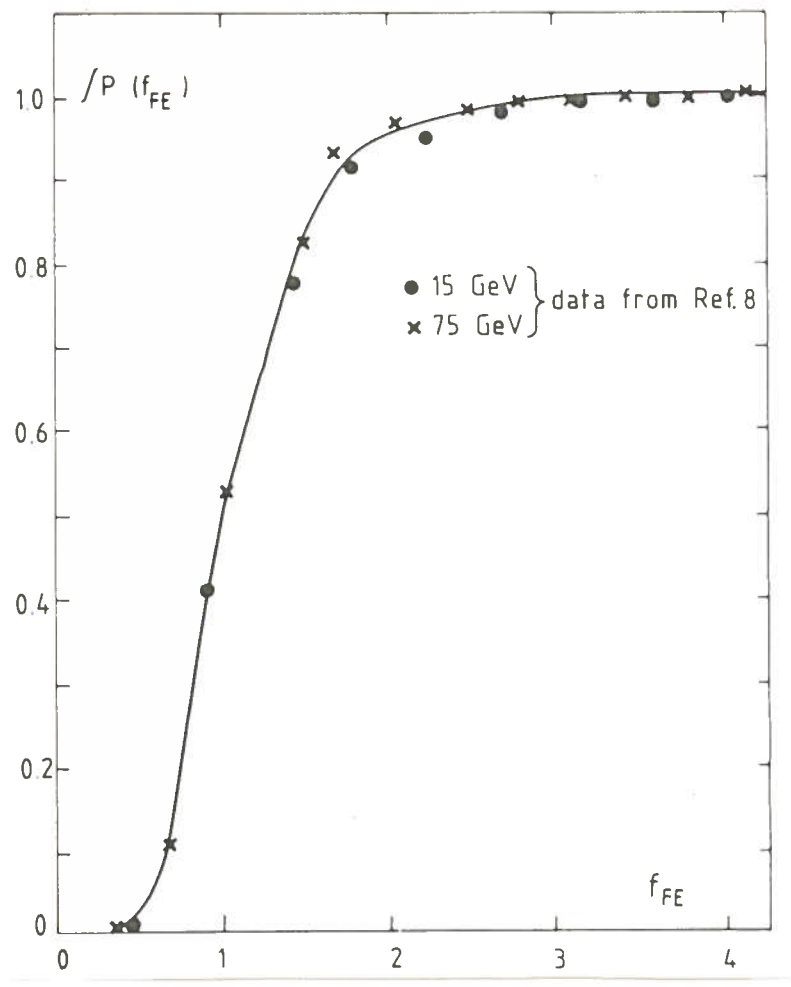

FIG. 8 - Integral distribution of the f ratio for hadronic showers in iron. f is the ratio between the center of gravity of a generic shower and the center of gravity of the mean shower. The solid line represents the curve used in the simulation method.

In order to evaluate a similar distribution for lead, the average shower, described by eq. (1), was assumed to be a good approximation of the universal longitudinal profile. The generic shower profile can then be written as:

$$dE/dx = E\left[w(s/f)^{(\alpha_E-1)}\exp(-s\beta_E/f) + (1-w)(t/f)^{(\alpha_H-1)}\exp(-t\beta_H/f)\right] \qquad (3)$$

where, in respect to eq. (1), s and t are scaled by a factor $1/f$.

The f parameter was fitted for each shower by minimizing the following expression:

$$S = \Sigma(dep(x_i) - dep(x_i, f))^2 \qquad i = 1, \ldots, 4 .$$

$Dep(x_i)$ is the measured energy deposition in 4 different positions, and $dep(x_i, f)$ is the energy deposition calculated with the eq. (3) at the same position x_i (i. e. s and t).

The fit has an average (S/nD) = 0. 7.

The f distribution at 20 GeV is plotted in Fig. 9 while the integral f distributions at both 13 and 20 GeV energies are shown in Fig. 10. These distributions seem energy independent as the one in iron.

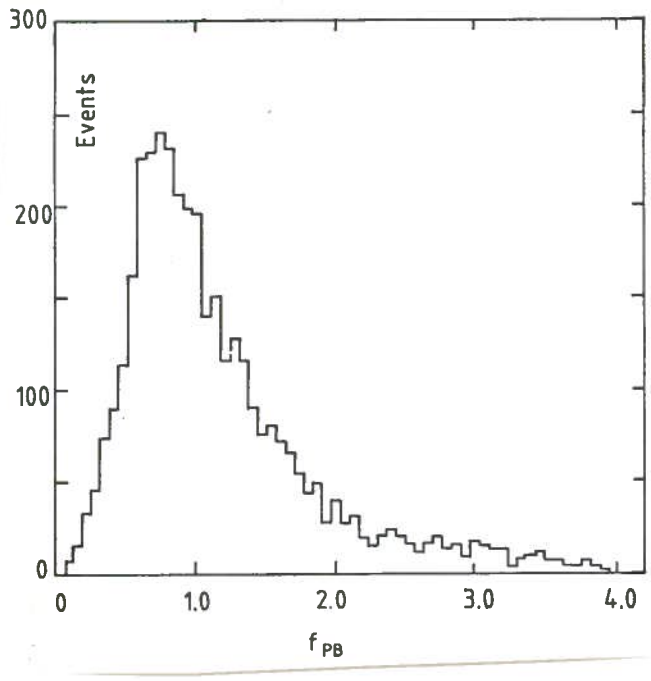

FIG. 9 - Distribution of the f ratio for hadronic showers in lead at 20 GeV. The distribution is derived from eq.(1) and from the assumption made in the text.

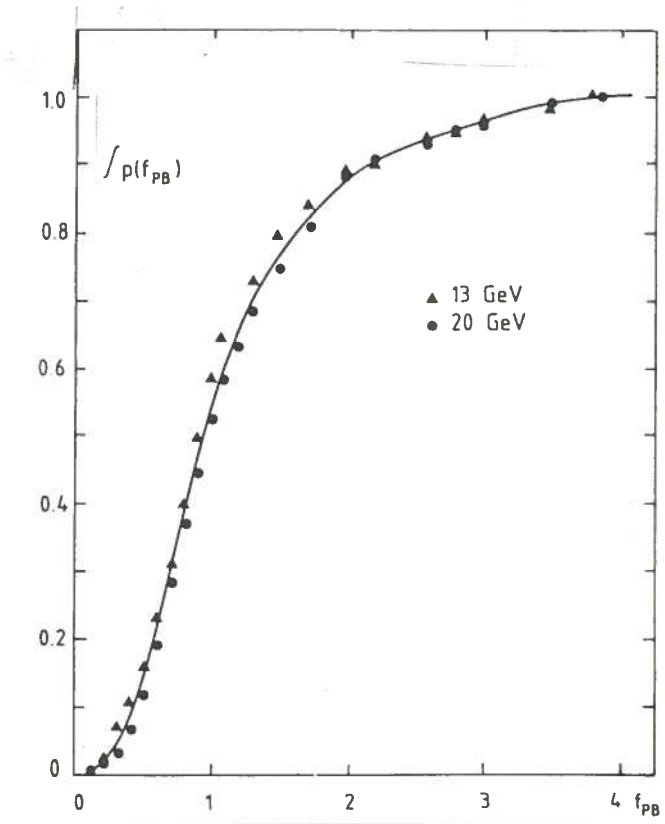

FIG. 10 - Integral distribution of the f ratio for hadronic showers in lead at 13 and 20 GeV. The solid line represents the curve used in the simulation method.

5. - SIMULATION

In order to reproduce the hadronic shower responce of the ring calorimeter a simulation method based on the eq. (1) was developed. The eq. (1) represents the average shower development. A real shower, however, fluctuates around this average because of the statistic nature of shower development. Therefore, some fluctuations were introduced in order to better describe the shower real behaviour.

Three kinds of fluctuations were considered:

a) Fluctuations in the shower origin with a probability distribution

$$P(x) = (1 - \exp(-x/\lambda_{ab})).$$

b) Fluctuations in the incident energy to introduce the energy resolution of the calorimeter. For the ring calorimeter we used a normal distribution with mean = E and sigma = $E\ (0.64/\sqrt{E} + 0.02)$ [4, 6] where E is the incident energy in GeV.

c) Fluctuations in the shower length based on the hypothesis of section 4. The f ratio was extracted, depending on the shower origin position, according to center of gravity distributions in lead or in iron. The value for t and s, used in eq. (1), were redefined as

$$t' = t/f\,, \qquad s' = s/f\,.$$

The energy normalization was obtained setting:

$$E = \int_0^x dE = E\left[wG(\alpha_E, \beta_E s) + (1 - w)\,G(\alpha_H, \beta_H t)\right]$$

where $G(\alpha, \beta)$ is the partial Γ function.

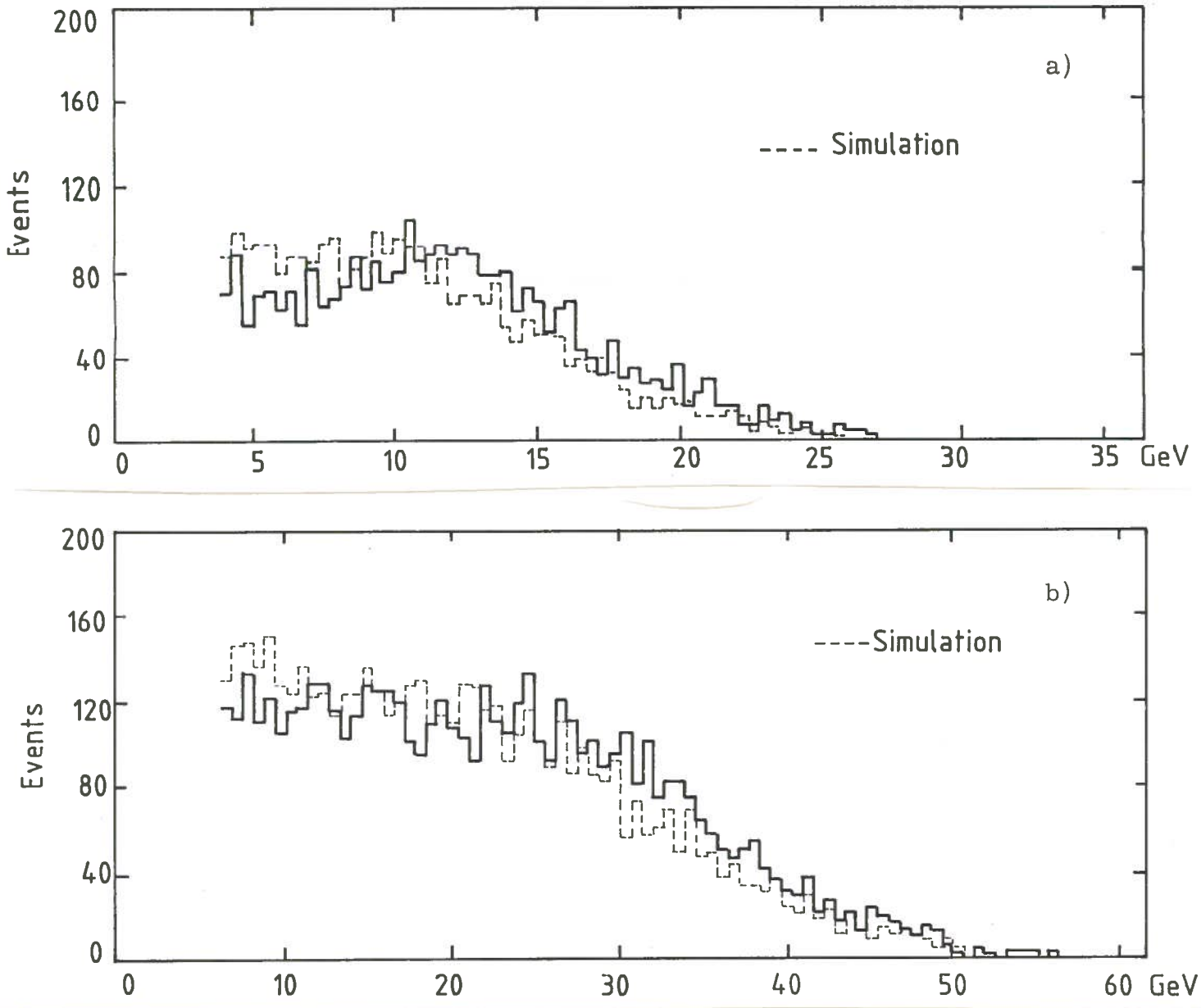

FIG. 11 - The measured and simulated energy deposition distributions in the electromagnetic section of the ring calorimeter: a) 16 GeV, b) 35 GeV.

The measured and simulated energy deposition distributions respectively in the e. m. section and in the hadronic section of the ring calorimeter without PPD are shown in Figs. 11 and 12. The same distributions with a prototype of the PPD ($8X_o$ thick) in front of the calorimeter are shown in Figs. 13 and 14. The agreement between the data and the simulation is satisfactory. Some discrepancies are found only when a little fraction of the incident energy is deposited in the hadronic calorimeter. This happens when the

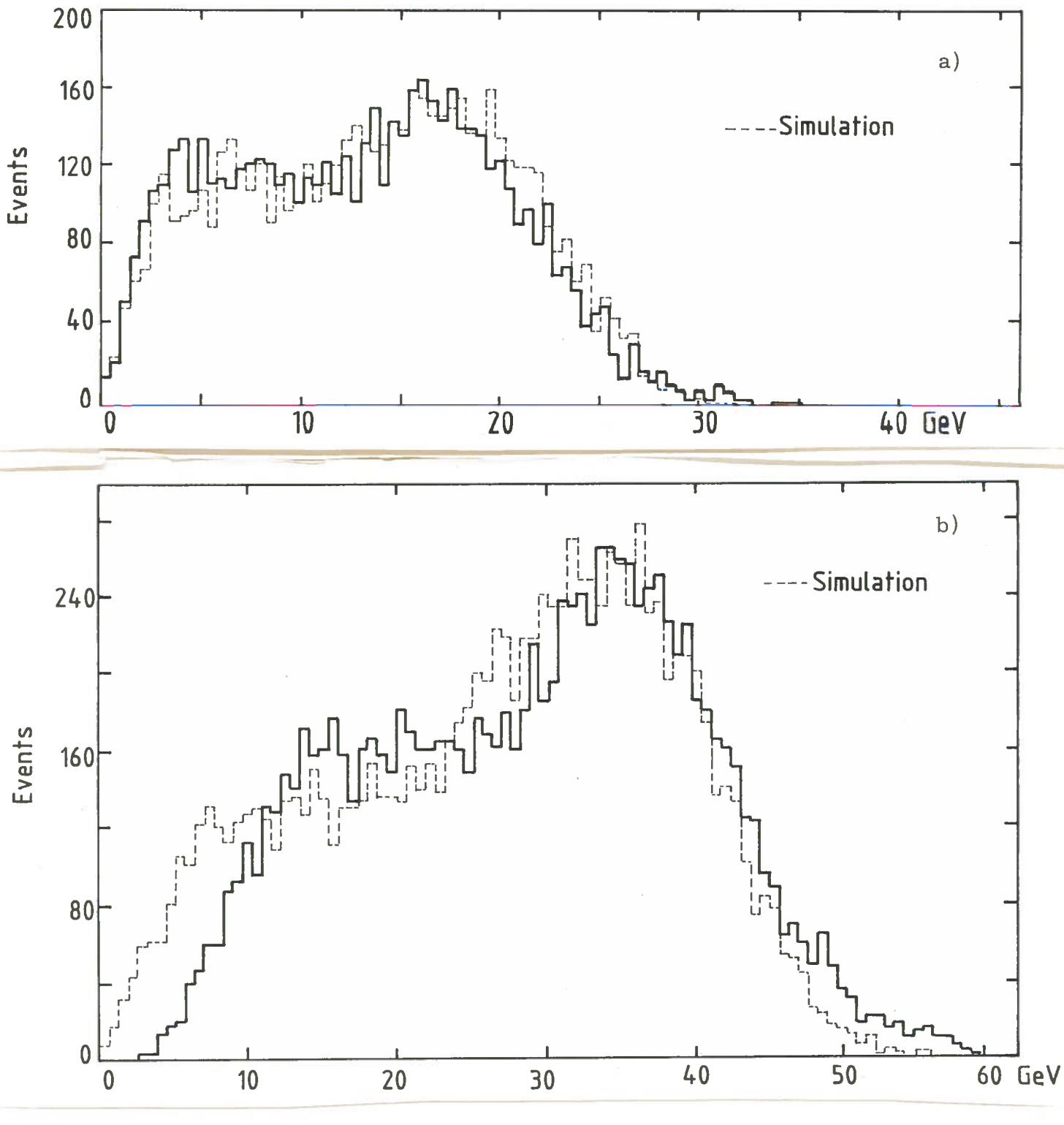

FIG. 12 - The measured and simulated energy deposition distributions in the hadronic section of the ring calorimeter: a) 16 GeV, b) 35 GeV.

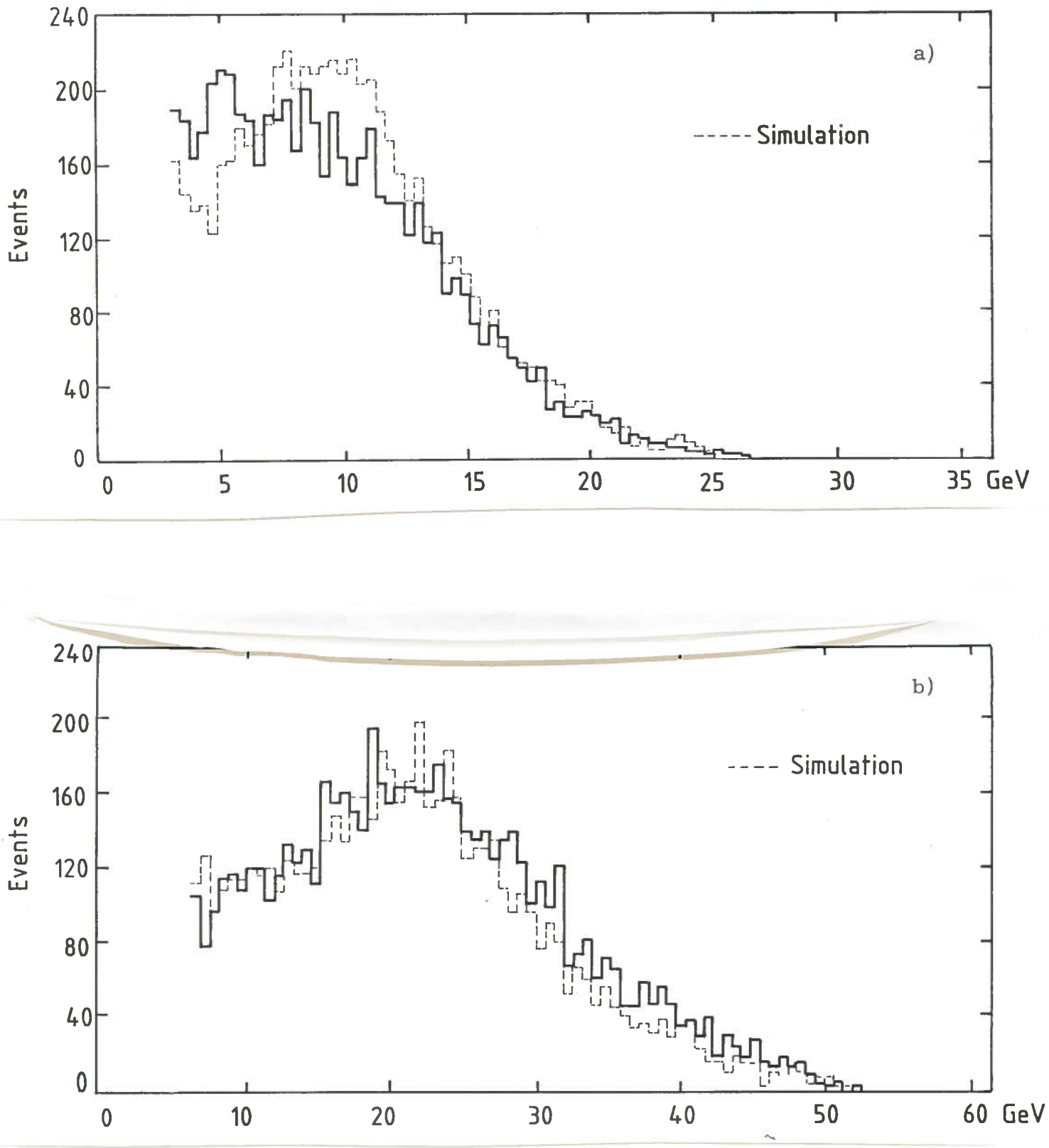

FIG. 13 - Idem to Fig. 11, but with $8X_o$ in front of the ring calorimeter.

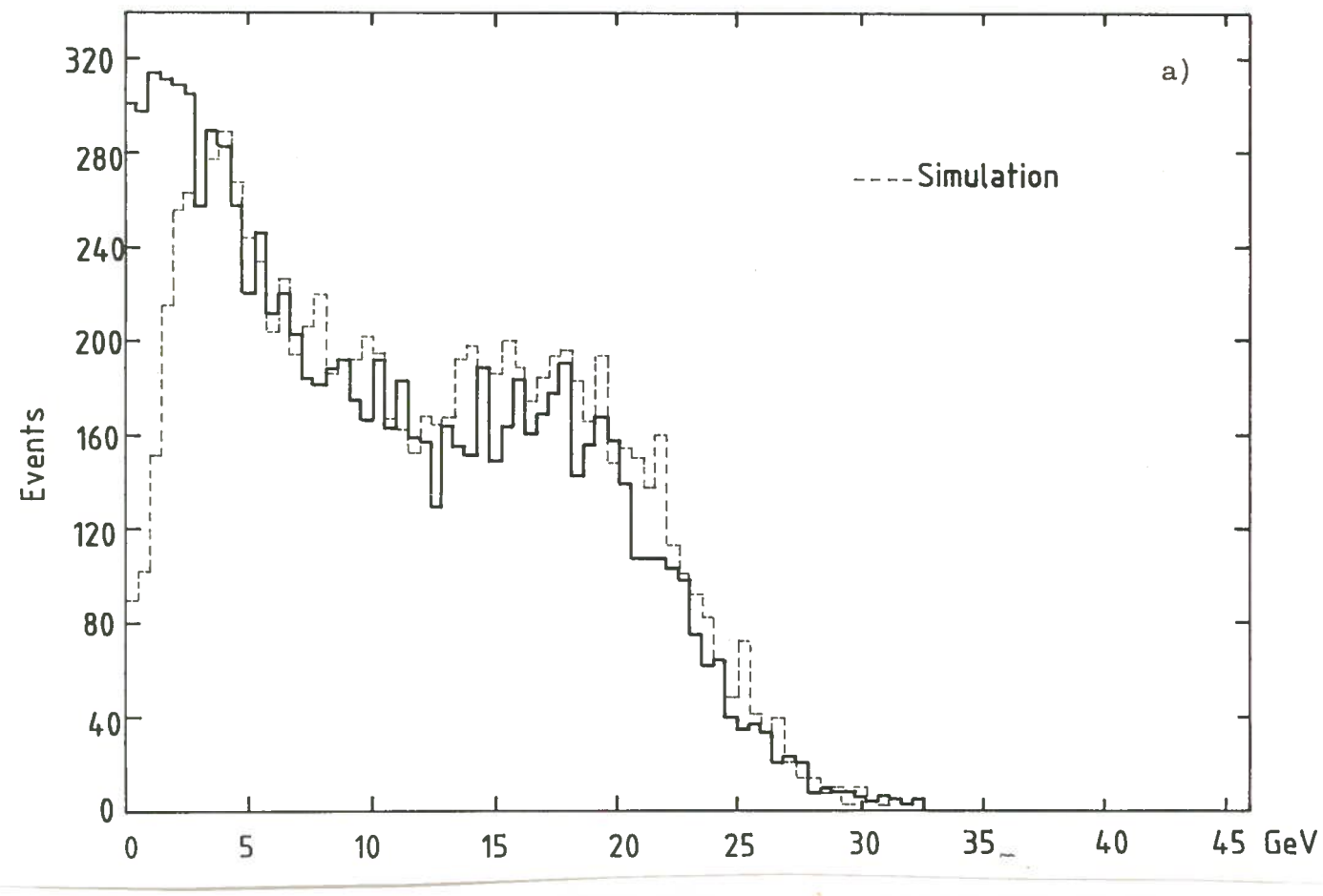

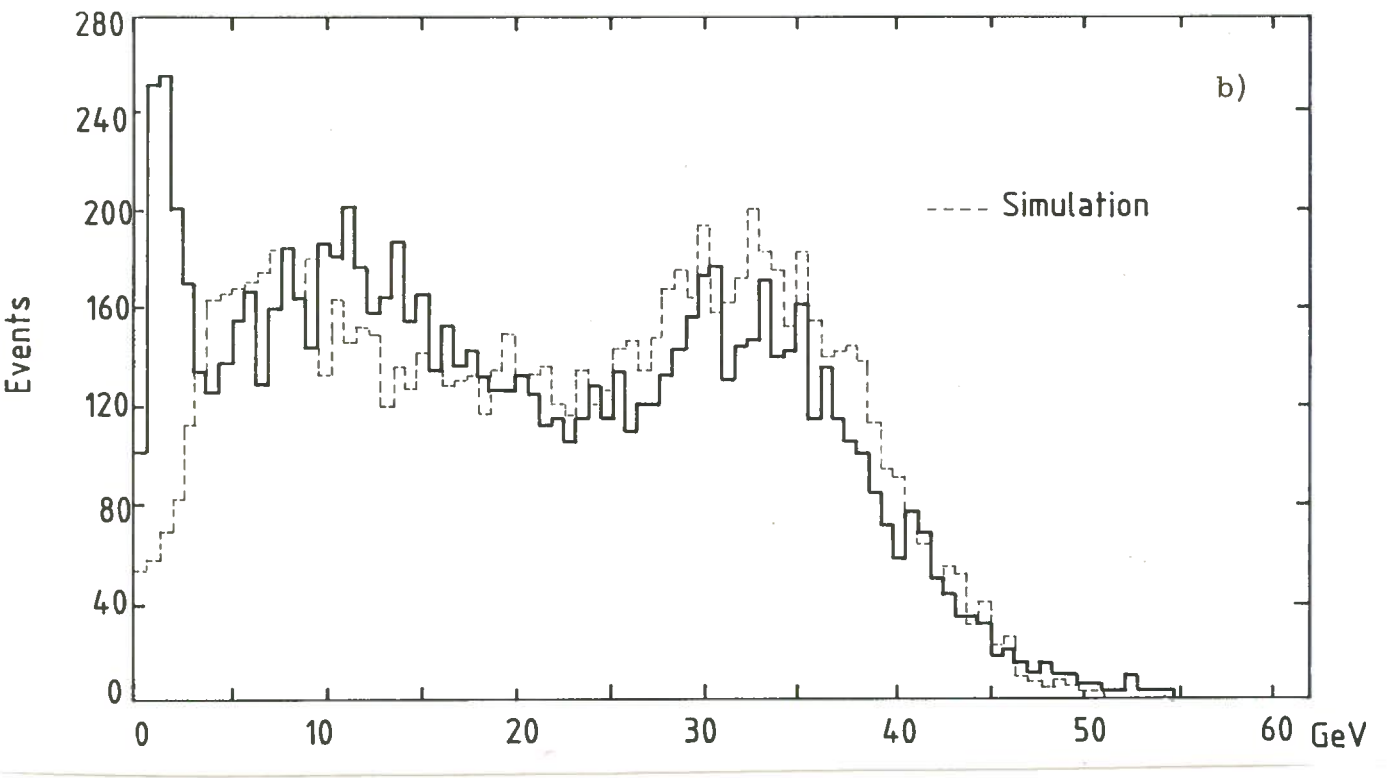

FIG. 14 - Idem to Fig. 12, but with $8X_o$ in front of the ring calorimeter.

shower starts in the first lead plates and deposits its tail in the hadronic calorimeter. This discrepancy may be due to insufficient knowledge about the shower tail.

Both the particle incident angle on the calorimeter front and the lateral spread of the showers have not yet been taken into account. We believe that these can also be introduced into the method by means of a similar procedure and at present we are working towards this goal. The approach described can prove very useful for a simulation of the response of calorimeter devices to hadrons produced in high energy interaction since it is not very computer-time expensive. Actually it takes only 0.5 sec of CPU time to generate 100 showers on a VAX-780 computer.

ACKNOWLEDGEMENTS

We would like to thank the NA24 collaboration for the support at CERN, our technical staff in Bari and in particular R. Ferrorelli and F. Ceglie for building the counters, M. Perchiazzi and A. Sacchetti for their significant contribution in the setting up of the equipment. We are also grateful to Dr. M. Tarantino for revising the English text.

REFERENCES

(1) - A. Grant, Nuclear Instr. and Meth. 131, 167 (1975).

(2) - T. A. Gabriel et al., Nuclear Instr. and Meth. 134, 271 (1976).

(3) - A. Bamberger et al., CERN/SPSC/80-83 P 151 (1980).

(4) - C. De Marzo et al., Nuclear Phys. B211, 375 (1983).

(5) - V. Artemiev et al., Paper presented at "Wire Chambers Conference", Wien, 1983.

(6) - C. De Marzo et al., internal note CERN/EP/NA24/KP/83, submitted to NIM.

(7) - V. Eckart et al., Nuclear Instr. and Meth. 155, 389 (1978).

(8) - M. Holder et al., Nuclear Instr. and Meth. 151, 69 (1978).

(9) - A. L. Sessoms et al., Nuclear Instr. and Meth. 161, 371 (1979).

(10) - R. K. Bock et al., Nuclear Instr. and Meth. 186, 533 (1981).

(11) - F. E. Taylor et al., IEEE Trans. Nucl. Sci. NS-25, 1, 312 (1978).

(12) - A. Benvenuti et al., Nuclear Instr. and Meth. 125, 447 (1975).